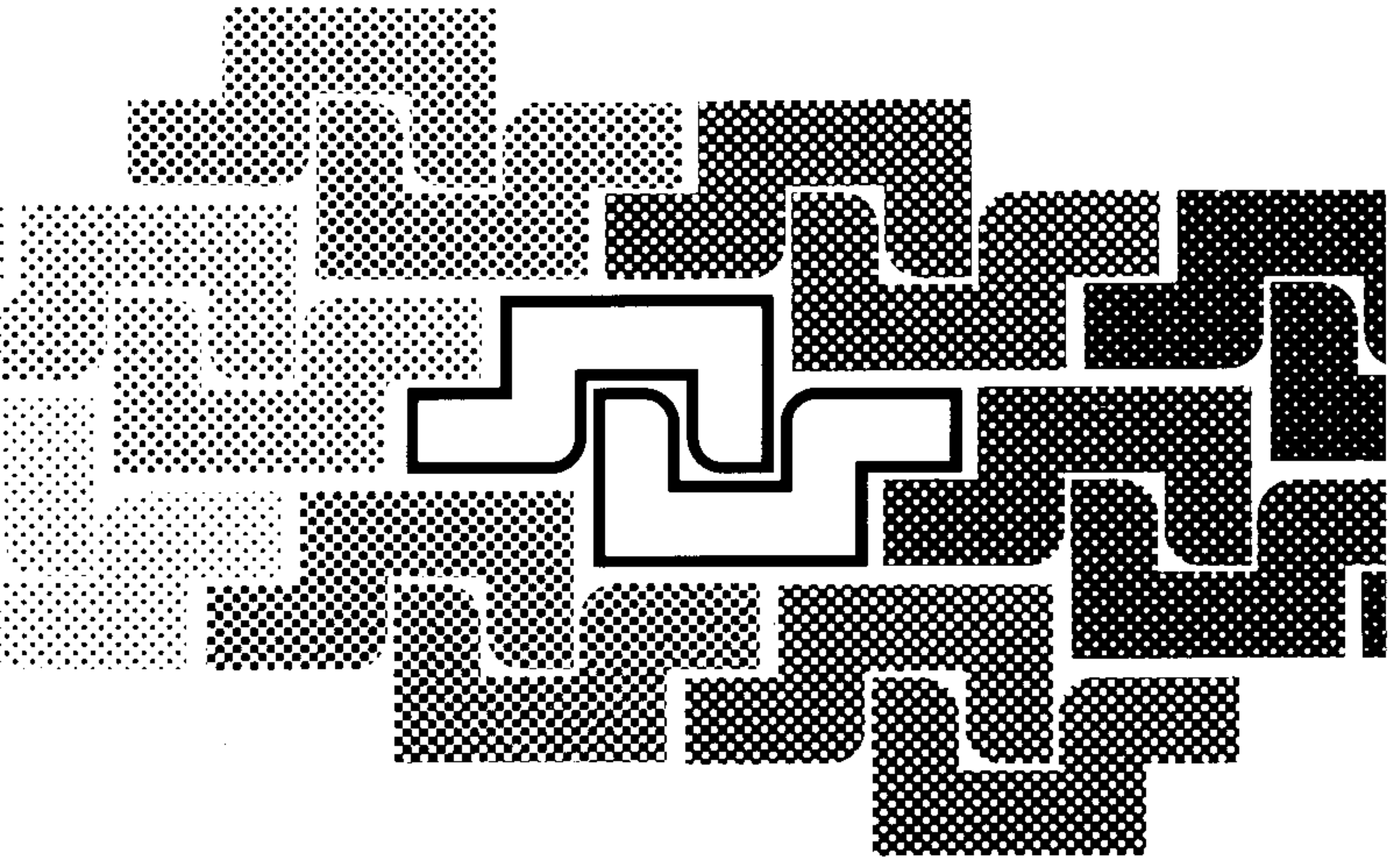


Nanostructured Magnetic Materials and their Applications

Edited by

Bekir Aktaş, Lenar Tagirov and Faik Mikailov

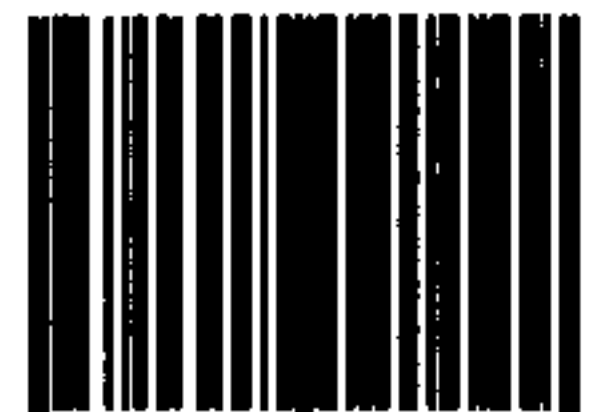
NATO Science Series



NATO Science Series
II. Mathematics, Physics and Chemistry

Kluwer Academic Publishers
Dordrecht/Boston/London

ISBN 1-4020-2004-X



9 781402 020049

MAGNETOIMPEDANCE OF THE NOVEL MAGNETIC NANOSTRUCTURES IN EXTRA HIGH FREQUENCY BAND: PHYSICS, TECHNIQUE AND APPLICATION

Sergey Tarapov

*Institute of Radiophysics and Electronics NAS of Ukraine, 12 Ac Proskura St., 61085,
Kharkov, Ukraine; e-mail: tarapov@ire.kharkov.ua*

Abstract: One of the promising areas for application of nanostructures is high-frequency electronic industry. Thus, the problem of study of nanostructures in the frequency band which coincides with the band of their application attracts today attention of experts. In given report the results of extra-high frequency (EHF) electromagnetic wave interaction with various layered nanostructures are discussed. The behavior of Giant Magnetoresistance (GMR) effect depending on the applied static magnetic field is compared with similar EHF-phenomenon - Giant Magnetoimpedance (GMI). We used the Electron Spin Resonance (ESR) technique at frequencies 10-40 GHz, 65-80 GHz and the non-resonance EHF technique at 40-140 GHz as main experimental methods of research. Examples of applications of GMI nanostructures under study for design of electronically controlled EHF-devices are discussed.

Key words: nanostructures, multilayers, Electron Spin Resonance, extra-high-frequency band

1. INTRODUCTION

Nanostructures appear to be promising materials for application in the Extra High Frequency (EHF) technology and design because their magnetic properties are rather sensitive to the influence of alternative current of this frequency band [1-3]. On this reason we studied the nanostructures (such as layered magnetic metallic systems) in the frequency band which coincides with the band of their prospective application by the Electron Spin Resonance (ESR) technique[5, 6]. In this paper the resumptive review of

researches performed in IRE NASU (Kharkov, Ukraine) and KhPI (Kharkov, Ukraine) is presented and results of the studies are analyzed.

2. SPECIMENS

We worked mainly with GMR multilayered (ML) structures $\text{Fe}(6 \text{ nm})/[\text{Co}(t \text{ nm})/\text{Cu}(d \text{ nm})]_8$ and $\text{Fe}(6 \text{ nm})/[\text{Co}(t \text{ nm})/\text{Cu}(d \text{ nm})]_{30}$ with magnetoresistance ratio of 5-10% [4,5]. The Co-layers thickness varied from $t=1 \text{ nm}$ to $t=4 \text{ nm}$. The Cu-layers thickness varied in the range d of 1.7 nm-7.4nm. The films have been produced using a combination of two methods: triode ion-plasma sputtering for cobalt and iron deposition and magnetron sputtering for copper deposition. The films have been deposited on non-cooled glass-ceramic substrates with specially prepared surfaces covered by amorphous oxide to diminish surface roughness. Multilayer samples under study were polycrystalline and exhibited rather well defined laminated structure according to data of X-ray diffraction and electron transmission microscopy of oblique cross-sections. Also it was proved that any detectable interfacial mixing in ML structures under study is absent. In more detail the procedure of manufacturing and physical properties of such multilayers is described in Ref. [7].

3. EXPERIMENTAL AND ANALYSIS

We used the ESR method to study the magnetic characteristics of the films [4]. ESR method allows to separate the contribution of both Fe - buffer layer and Co - multilayers to the magnetic structure of the system. A typical line shape [8], where two peaks ("sharp" - for Fe and "weak" - for Co) are presented is shown in Fig. 1. As the experimental data was detected in rather wide frequency range 20-75 GHz, we were able to get resonance field - resonance frequency dependence with high enough accuracy (Fig. 2). More detailed procedure is described in [2, 6, 8]. Here we note only that using known Kittel formulas for these dependencies we determined a dynamic magnetization for each component of the multilayered structure (for Co and Fe) separately.

The data on dynamic magnetization for all set of specimens allow to make general conclusion that the specimens with largest Cu-layer thickness ($t=7.4 \text{ nm}$) have the largest magnetization values as well. At the same time, the magnetization is almost independent from Co-layer thickness.

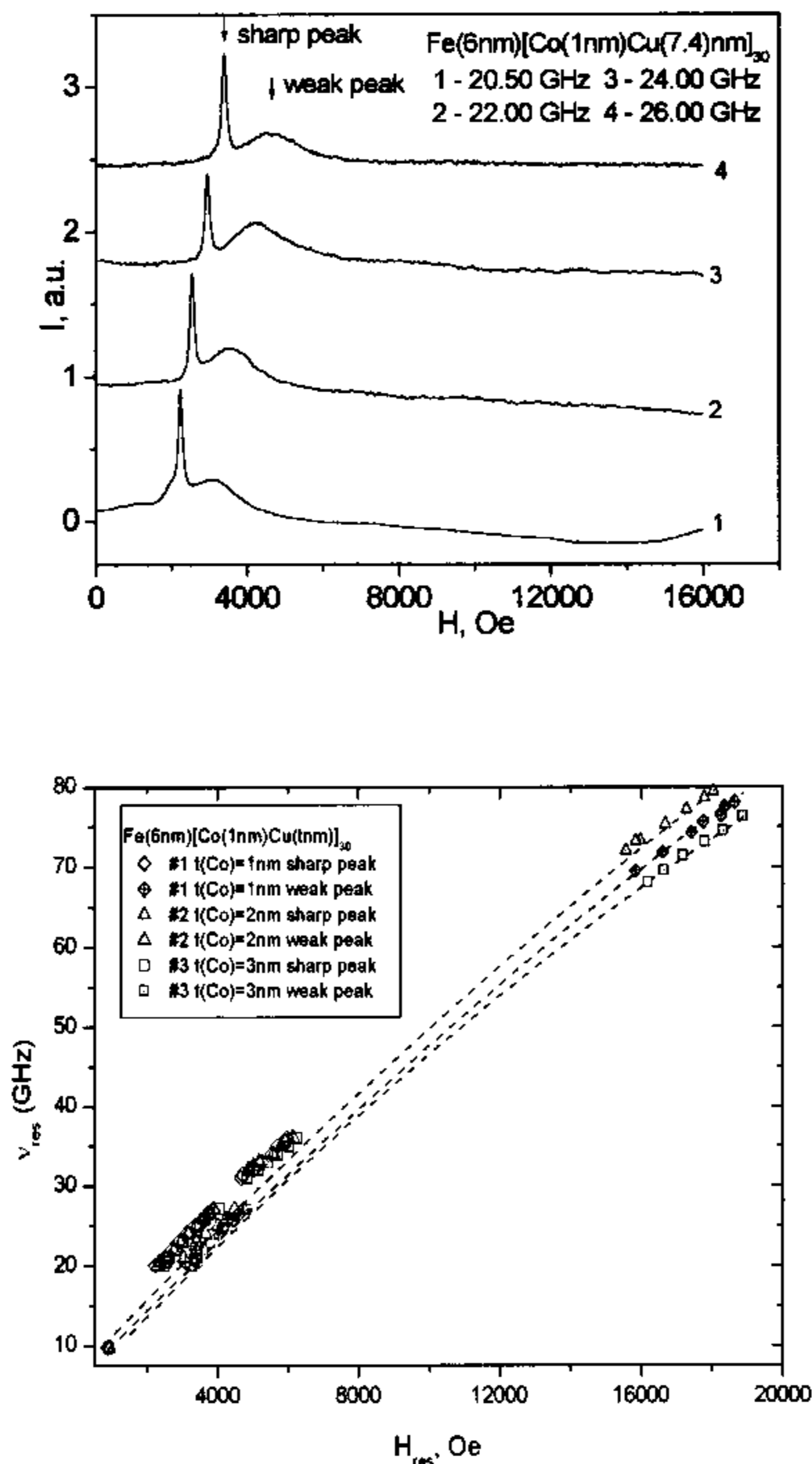


Figure 1. ESR data for Co/Cu multilayers: a) Typical ESR-line shapes for Co (weak peaks) and Fe (sharp peaks) in the Fe(Co/Cu) multilayers in millimeter waveband; b) Resonance frequency-field dependence.

Another, more important conclusion is that the multilayered nanostructures with large magnetization magnitudes are more perspective (suitable) for the application. Because of this, with increase of the magnetization magnitude the external magnetic field magnitude, at which the GMI effect occurs, decreases. So we can suppose that multilayers with

highest distances between Co layers are most suitable for EHF application. Of course, this distance should not be larger than that at which interlayer exchange interaction is noticeable.

In order to investigate in detail the DC-resistance behavior in presence of the external magnetic field, the dependence $\Delta R/R = f(H)$ (Fig. 2a) was detected during the static experiments. Besides, the same characteristics have been detected for AC currents, i.e. for the frequencies $f \sim 30-140$ GHz. An interesting result was revealed, that the behavior of the transmission coefficient (T) of the EHF wave, propagating through the ML structure (i.e. $\Delta T/T = f(H)$) in the entire frequency band 30-140 GHz, completely repeats the same dependence for DC-resistance: $\Delta R/R = f(H)$ [8]. The dependencies of such type are shown in Fig. 2b. Let us note that T coefficient is in direct proportion to the EHF impedance \dot{Z} within the accuracy of the experiment. Characteristic points on these graphs are the static field magnitudes H_m (the field of maximum magnetic disordering of the ML structure ≈ 200 Oe) and H_j (the field at which the domain walls start to rotate ~ 70 Oe).

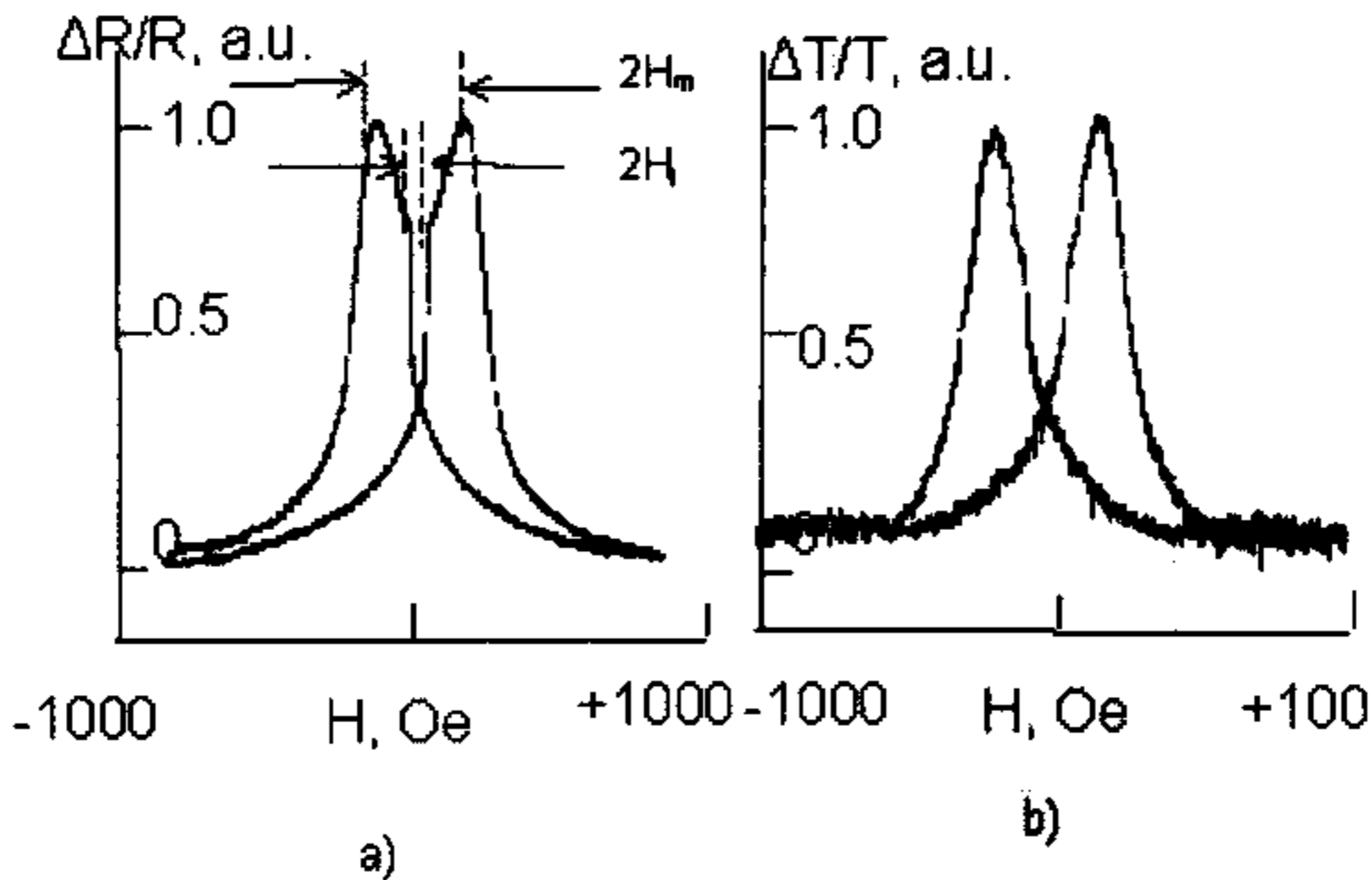


Figure 2. GMR (a) and GMI (b) responses for Fe(Co/Cu) nanostructures: a) DC response b) AC response at 120 GHz.

The dependence presented in Fig. 2 is of hysteresis type. The curve that describes the magnetoresistance variation when the static magnetic field magnitude changes from the negative magnitude to positive one is bilaterally symmetrical to the curve that describes the reverse variation of the static field. The magnitude of this hysteresis equals 200-300 Oe. As it is known

this phenomena is defined by the domain type of the magnetic structure under study.

We studied this hysteresis in small area of variation of external static magnetic fields in order to determine the optimal conditions for application of ML nanostructures in high-frequency technologies. As a result the so-called "partial" hysteresis (Fig. 3. position 1) on the EHF dependence $\Delta T/T=f(H)$ has been detected. In Fig. 3 the segment of $\Delta T/T=f(H)$ dependence is presented for the case when the reverse trace of the curve is started from the field magnitude close to $+H_m$. In such case one can observe typical hysteresis dependence with a hysteresis magnitude of about 200 Oe.

The remarkable fact is that the reverse lines on the partial hysteresis (1) for the field, which is scanned in small band ~ 50 Oe, are located closely to direct lines, so the loops of "partial" hysteresis are rather small and have approximately linear type of the field dependence. At the same time the type of the impedance variation on the external H -field have the similar character as for the main impedance.

Another interesting result is that thorough study of the curves presented in Fig. 3 allows to state that linear segments of $\Delta T/T$ dependence take place. This result is rather valuable from the point of view of ML application as EHF amplifying-transforming devices.

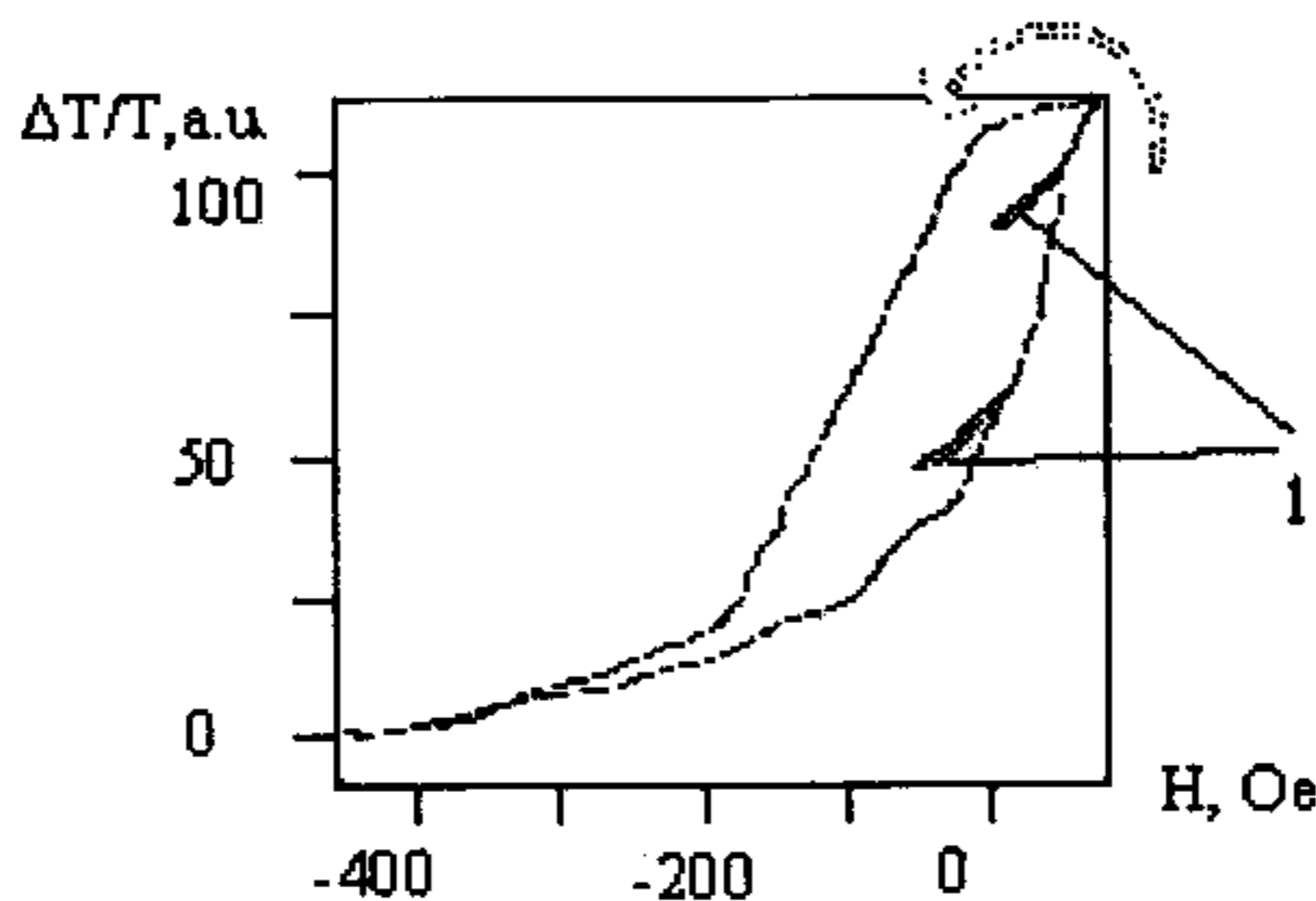


Figure 3. The general hysteresis and the "partial" (1) hysteresis of the magnetoimpedance for the multilayered nanostructures Fe(Co/Cu) for $f=44$ GHz.

On the basis of the results described above it is necessary to make certain conclusions which determine the possible areas of application nanostructures (particularly - multilayers):

1. $\Delta T/T = f(H)$ repeats completely the $\Delta R/R = f(H)$ dependence in the entire frequency band $f \sim 30-140$ GHz.
2. The relaxation times of the processes, which are responsible for the magnetoimpedance have values $\tau \approx f^{-1} \leq 10^{-11}$ s.
3. The linear-type dependence and the small width of partial hysteresis allows to assume that while applying the external field H , which varied by a certain time-law, it is possible to reveal the similar time dependence for the impedance.
4. Specimens with largest magnetization are most promising for the GMI applications in EHF band.

Thus the nanostructures under study are rather promising for the EHF technology applications. Let us note that main directions of the researches, which should overcome disadvantages of these structures are:

- to increase the $\Delta T/T = f(H)$ magnitude up to (30-50%)
- to increase the magnetization and anisotropy fields in order to decrease the external field of the electron spin resonance.

4. APPLICATIONS OF NANOSTRUCTURES FOR EHF DESIGN

In spite of some imperfections mentioned in previous chapter ML nanostructures seem to be promising elements for the EHF-band application due to reasons listed above.

The remarkable outcome one can make from them is that the usage of these ML nanostructures allows to arrange electrical/electronic management of their EHF parameters in contrast to mechanical ones (as it takes place in the majority of contemporary devices). Let us note that this is a traditional way of technology: to replace the mechanical management of the device with the electronic one. This way leads to improvement of the reliability of the devices and to increasing the accuracy of processes control.

We would like to present below several directions conducted by our Laboratory in order to describe possible applications of nanostructures in some areas of EHF design.

4.1 Attenuator. Frequency Filter

An effective frequency filter of millimeter (mm) wavelength band can be created on the base of Disk Dielectric Resonator (DDR) [11] with flat surface covered with GMI multilayer.

A model of such filter on the cryogenic test-bench is presented in Fig.4. Several types of disk dielectric resonators (DDR) have been manufactured for the electro-dynamical test experiments. We used high quality materials: isotropic polycrystalline quartz; single-crystal quartz and single-crystal sapphire. Taking into account the mentioned frequency band we calculated their geometrical parameters such that it will have in their spectra the whispering gallery modes. The radius of the DDR is about $R \approx (4-7) \cdot \lambda \cdot \epsilon^{-1/2}$ (λ is the wavelength; ϵ is the DDR material permittivity). The thickness of DDR is about $t \approx 0.5 \cdot \lambda \cdot \epsilon^{-1/2}$. The GMR multilayer is deposited on the both of flat surfaces of the disk. The disk dielectric resonator with ML placed between two coupling waveguides shown in Fig. 4a. An external static magnetic field $H_s \sim 300$ Oe is created by the coil located under the DDR.

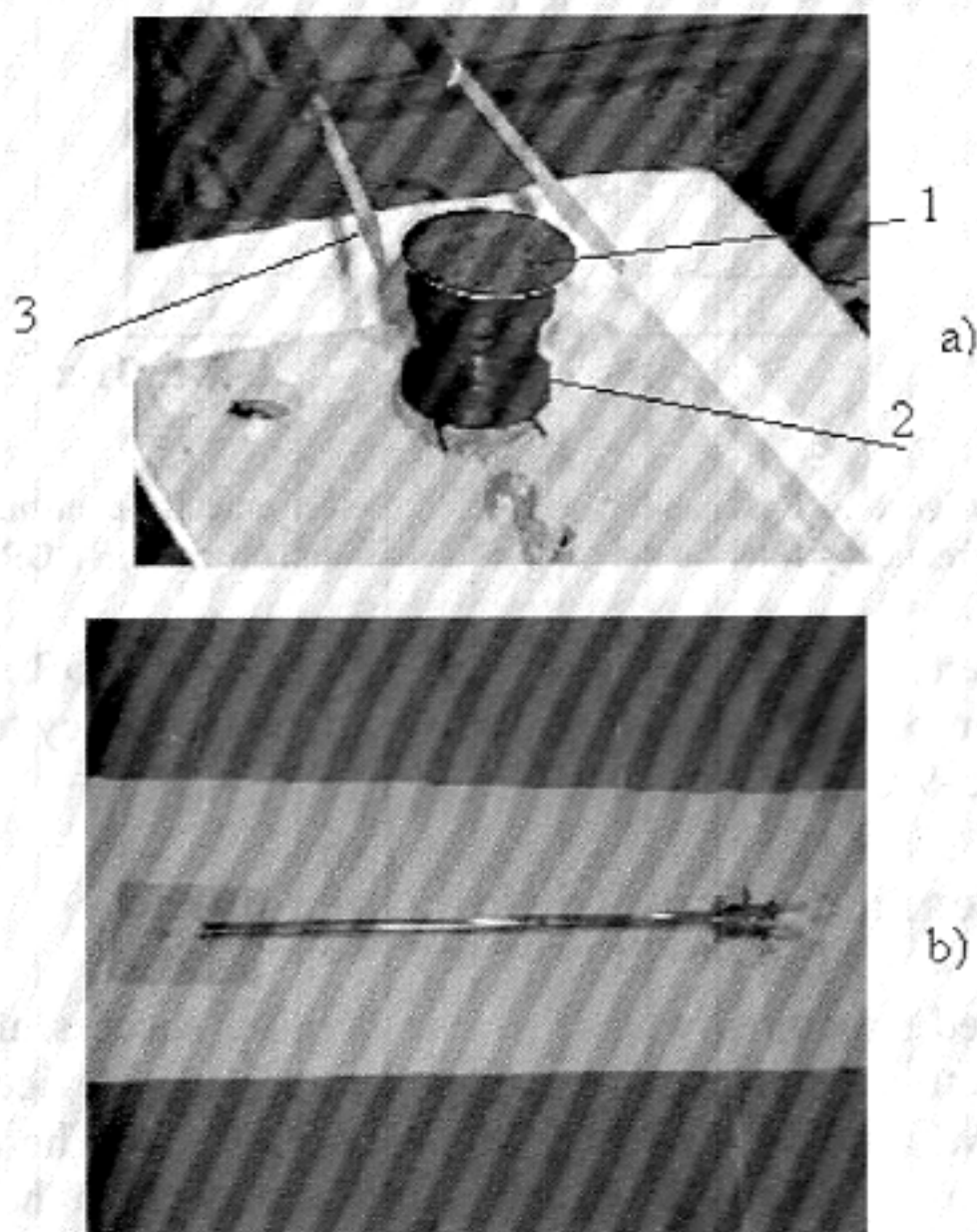


Figure 4. Modeling of the EHF filter based on the GMI multilayer structures: a) DDR covered by GMI multilayer with quartz waveguides; b) DDR placed on the cryogenic module for experiments at $T < 4$ K.

The principle of operation of such EHF filter is based on the fact that DDR has rather high quality factor for "whispering gallery" oscillation modes:

$Q \sim 3-5 \times 10^4$ at the room temperature and $Q \sim (1-3) \times 10^5$ at liquid helium temperatures. This provides the width of DDR's resonance curve (Fig. 5) of order $\delta f \approx 30$ MHz for $T=300$ K and $\delta f \approx 2-7$ MHz for $T < 4.2$ K. The transmission coefficient changes its magnitude $\delta T \sim 70\%$ while the frequency of the input signal varies in the band of $f_0 \pm \delta f$. In order to realize the electronic tuning/control of the filter it is necessary to vary the static magnetic field. As a result, the flat boundary of DDR changes its impedance and the eigen-frequency of the oscillation changes.

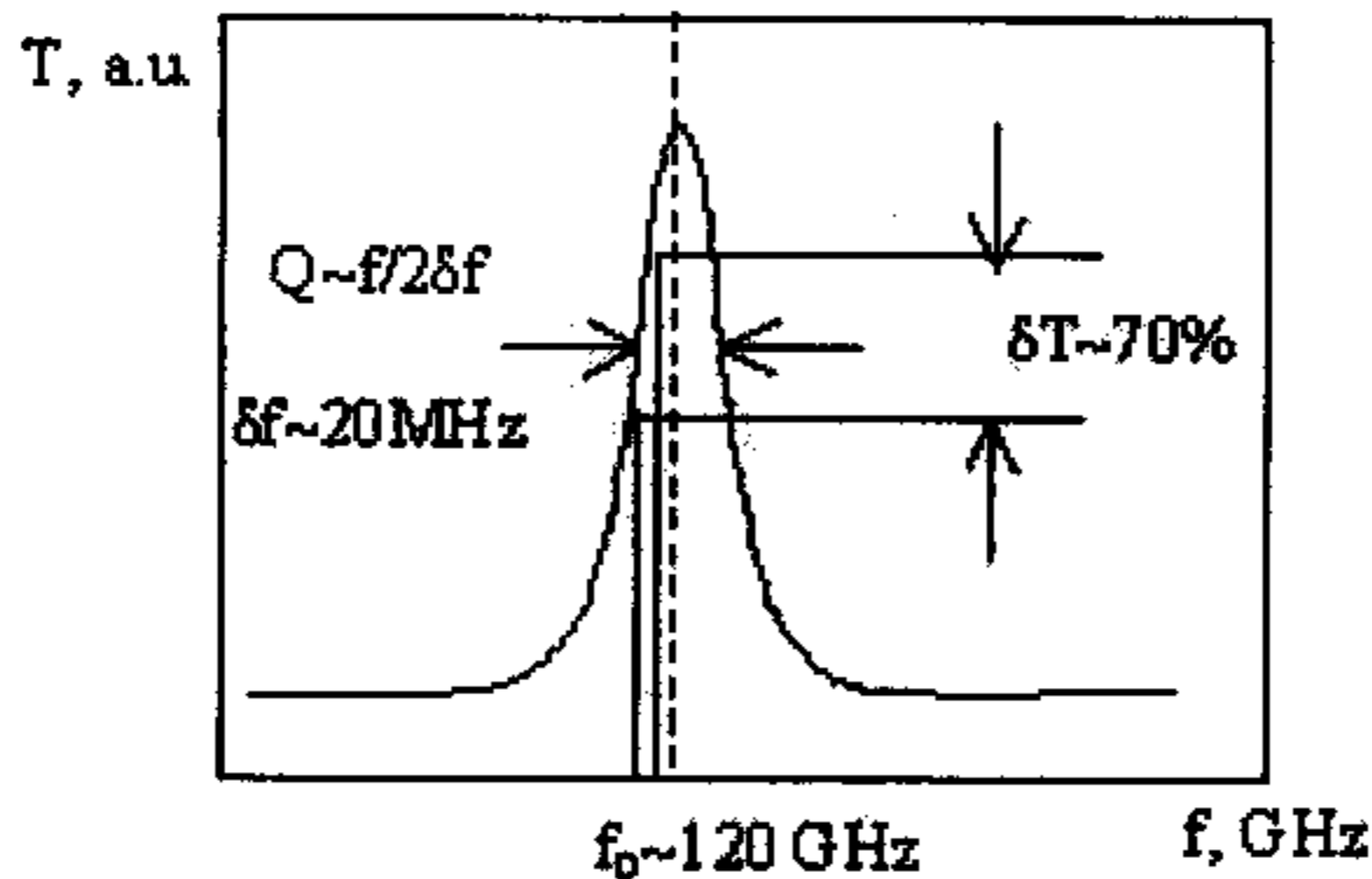


Figure 5. Resonance curve for the electronically controlled frequency filter on the GMI structure implemented in DDR.

Thus, one can shift the resonance frequency f_0 of the DDR in the range of about 5-7%. For example, in the 150 GHz band the frequency tuning range is approximately 5-9 GHz.

4.2 Antenna design (Griding - structure)

The multilayered structures with GMI can be used successfully in antenna design. An electrically managed phase-locked antenna device designed on the basis of GMI multilayered strips is shown in Fig. 6. The ML-strips are located in such a way that they form an antenna array [9]. When the incident

wave with the wave vector \vec{k} falls on the array at some angle θ_I , it excites the reflected wave propagating at the angle θ_R . The θ_R angle is defined by the geometrical parameters (the width) of the strips and by high-frequency

currents \vec{J} distribution in the strips as well. Strips are under the influence of the static magnetic field, produced by conventional wire conductors (2) with the DC currents located between ML-strips (1).

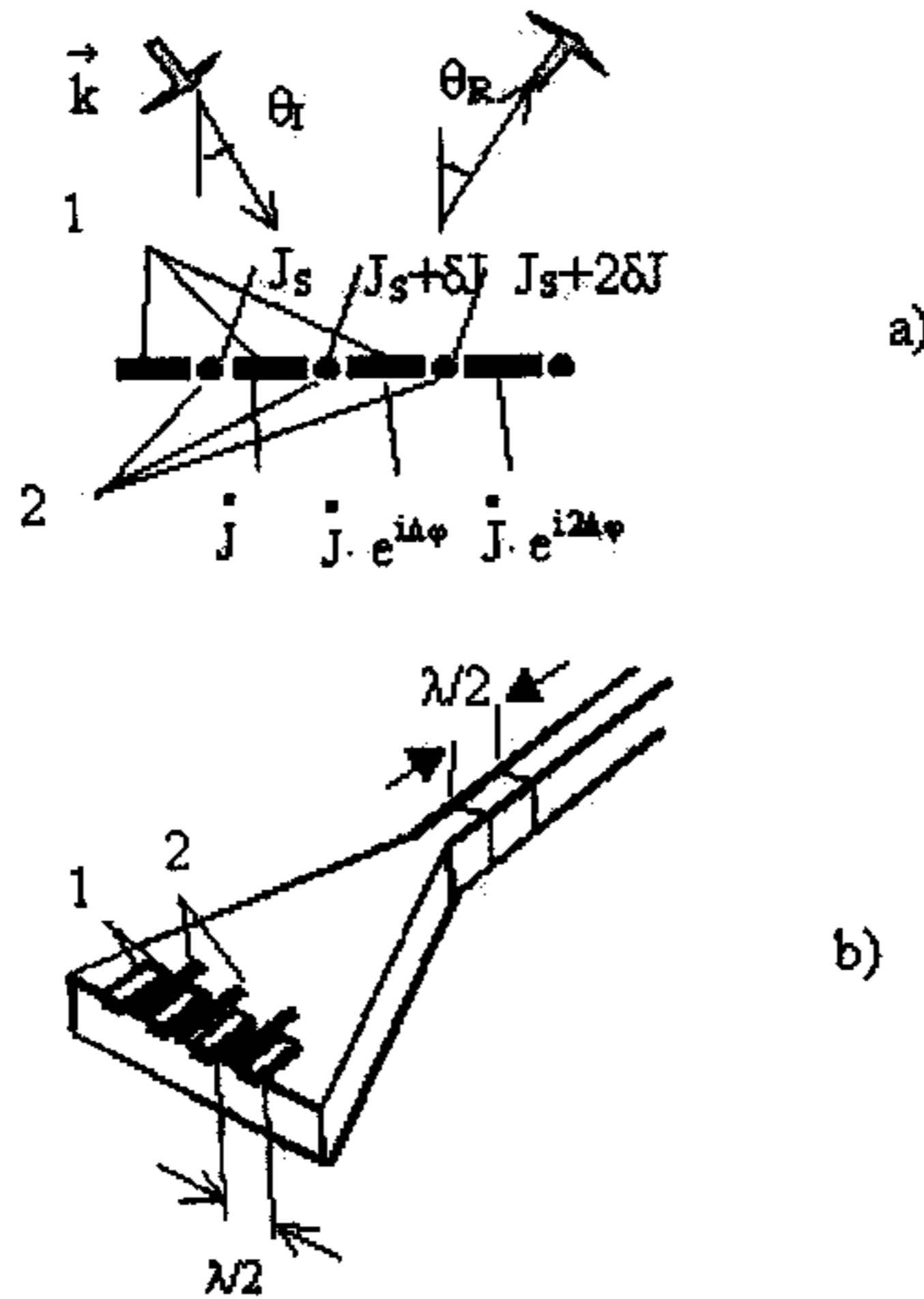


Figure 6. Phased-locked antenna array on the GMI elements.
 a) Principal flow chart b) design of the horn antenna array.

The distribution of static currents is presented in Fig. 6a. Variation of the static current on dJ leads to the variation of the static magnetic field created by these wires by some δH value. In its turn, it calls a definite phase shift ($\Delta\phi$) in AC currents which are excited in ML strips. Thus, it is possible to manage the EHF-currents distribution in the ML-strips while changing the DC current in the wires. Due to this a certain phase shift between EHF-currents in the strips can be provided. Following the known rules [9] of the phase-locked antenna-arrays design it is possible to arrange an electronical spatial scan of the antenna pattern. It is possible to change the angle of directivity of such antenna array varying the distribution of DC - currents amplitude (δJ).

In Fig. 6.b the model of the horn antenna combined with the GMI multilayered array providing the scan of the angle of radiation is presented as well. Preliminary experiments demonstrated the possibility to vary the antennas angle of radiation by the magnitude of about $\alpha \sim 5^{\circ}-9^{\circ}$.

4.3 EHF amplifying devices

On the reason of very small relaxation times of GMI processes $\tau \approx 1/f \approx 10^{-11}$ s, it is possible to employ ML structures in the area of amplifying (both linear and non-linear) radio-signals in the band 20-150 GHz [10].

4.3.1 Transistor. (The "linear" GMI-EHF-device)

The electromagnetic structure (resonator, waveguide, etc.) covered with the GMI nanostructure can be considered as a transistor-type device of the EHF band. The principle of such transistor operation is presented in Fig. 7. Here the first (increasing) segment belongs to the $\Delta T/T = f(H)$ dependence of GMI structure is shown.

Let us choose an EHF resonator included the GMI structure as an active element. For example the Disk Dielectric Resonator (Fig. 4) can be used.

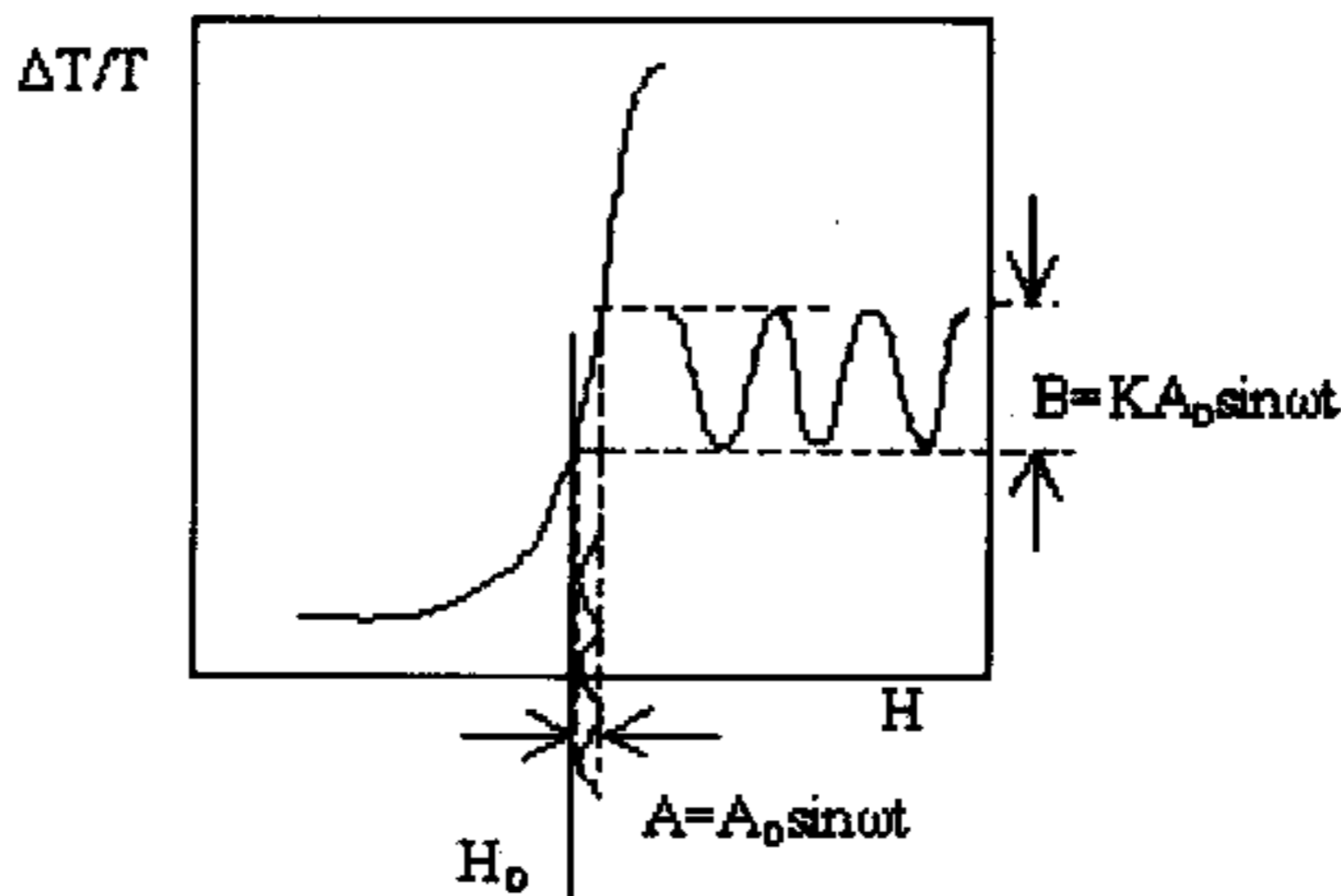


Figure 7. Principle of transistor on GMI phenomenon design.

Then let us choose the linear fragment of the $\Delta T/T = f(H)$ curve such as it presented in Fig. 7. In other words let us apply to the GMI - element located in electrodynamical structure the external static magnetic field of the definite value H_0 . Then impose the "information" EHF signal ($A = A_0 \cdot \sin \omega t$) with some amplitude (A_0) on the external magnetic field. Here ω belongs to the GHz band. It is evident from Fig. 7 that the variation of T follows this signal under the same harmonic law ($B = K \cdot A_0 \cdot \sin \omega t$) with the accuracy restricted only by linearity of the segment choused. Here the amplification coefficient (K) is defined by the slope of $\Delta T/T = f(H)$ curve.

4.3.2 Harmonic generator. The "non-linear" GMI-EHF-device

The same principle is the basis of the design of device which uses non-linear properties of GMI nanostructures, i.e. - harmonic generator. Let us note that the principle of devices of such kind, based on ferrites properties, is used in the microwave radio science for a long time. But in the given case when the ML structure is the active element, the external magnetic fields values (500 Oe instead 5000 Oe), required for its operation, are noticeably lower. The ML structure shows much smaller high-frequency loss in comparison with the traditional ferrite system, due to the physical nature of the materials.

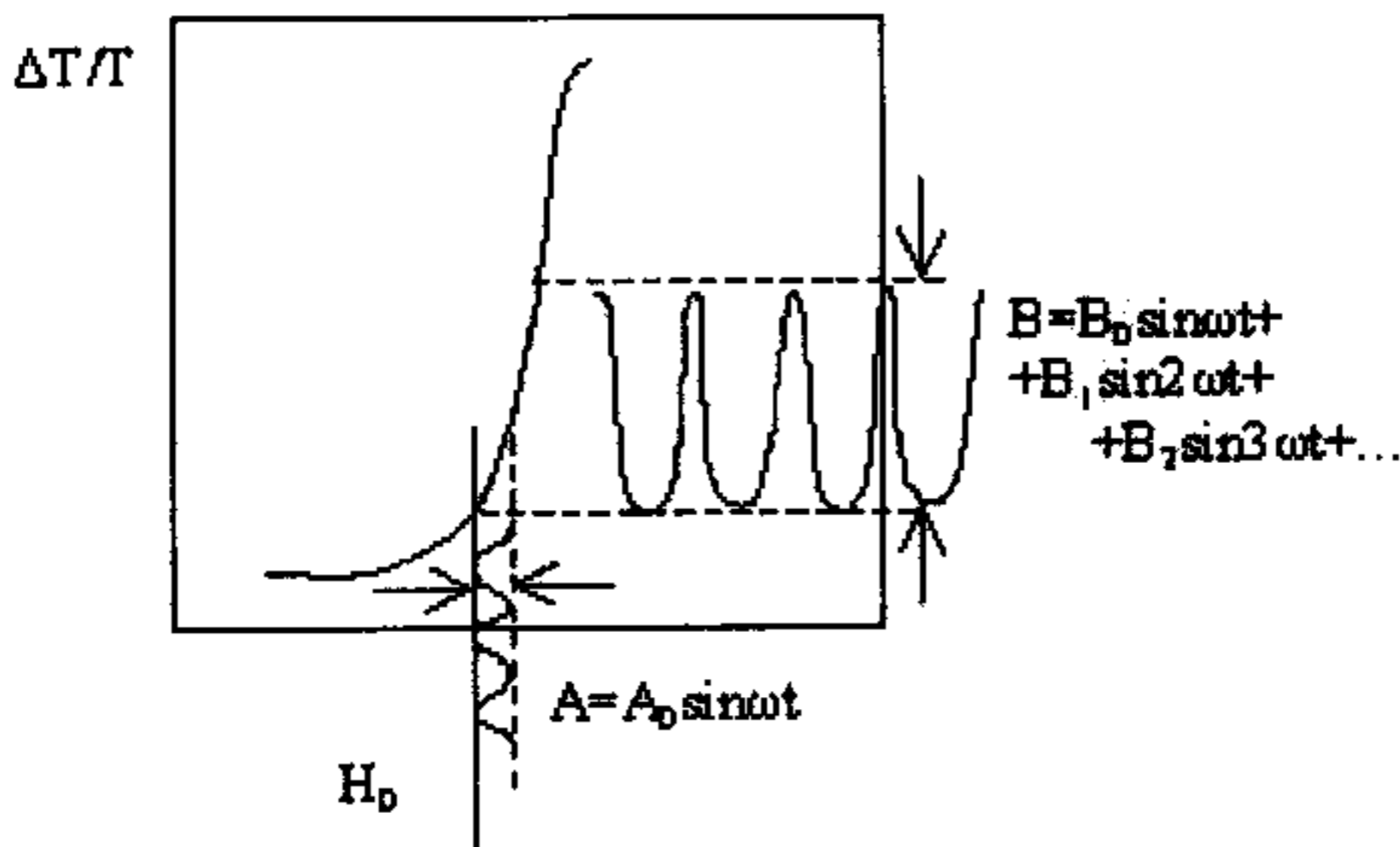


Figure 8. Principle of GMI EHF harmonic generator

Let us take the same DDR resonator covered with the GMI multilayer as it was described in the previous chapter. Then impose some external static magnetic field H_0 . Now let us apply the harmonic signal not to the linear segment of $\Delta T/T=f(H)$ but to some essentially non-linear segment as it is shown in Fig. 8. In such a case notwithstanding the applied signal is a harmonic one with the frequency ω the resulting signal $\Delta T/T=B(t)$ acquiring essentially non-harmonic character. In the given case it can be presented by a Fourier series of signals ($B=B_0 \cdot \sin \omega t + B_1 \cdot \sin 2 \omega t + B_2 \cdot \sin 3 \omega t + \dots$) with frequencies: $\omega; 2\omega; 3\omega; 4\omega \dots$ etc..

5. CONCLUSIONS

Thus, using the multilayered nanostructures designed for application in the EHF, it is possible to affirm that the GMI nanostructures are promising

elements which can be a basis for the electronically controlled Extra High Frequencies devices. Electrical (instead of the mechanical) type of control of the elements properties provides increasing of reliability, reproducibility and accuracy of EHF elements and devices. Short relaxation times of the tuning process, $\tau \sim 10^{-11}$ s, provide operation of such devices at frequencies at least not smaller than $f \sim 140$ GHz.

The work is partially supported by STCU grant #1916.

REFERENCES

1. A.B.Rinkevich, L.N.Romashev, V.V.Ustinov, JETP (2000) 117, N5, 960.
2. D.P.Belozorov, V.N.Derkach, S.I.Tarapov etc., Int. J Infrared Millimeter Waves, (2001) 22, N11, 1669.
3. A.Ludwig, M. Tewes, S. Glasmachers, etc.M. Lohndorf, E. Quandt, J. Magn. Magn. Mater, (2002) 242-245, 1126.
4. S.Tarapov, Basic of High-Frequency Electron Spin Resonance Experiment at Very Low Temperatures, Publ. Center of GIT, Gebze, Turkey, (2000) 93p
5. V.N.Derkach, S.V.Nedukh, A.G.Ravlik, I.G.Shipkova, S.T.Roschenko, S.I.Tarapov, Radiophysics and Electronics, (2002) 7, N1, 115.
6. D.P.Belozorov, V.N.Derkach, S.I.Tarapov, Foreign Radio Electronics. Advances in Modern Radio Science (2002) 12, 48.
7. S.T.Roschenko, A.G.Ravlik, I.G.Shipkova, Yu.A.Zolotarev, Phys. Met. Metallogr. (2000) 90 N3, 58.
8. D.P.Belozorov, V.N.Derkach, S.V.Nedukh, A.G.Ravlik, S.T.Roschenko, I.G.Shipkova, S.I.Tarapov, F.Yildiz, Intern. Journ. of Infrared and Millimeter Waves, (2001) 22, N11, 1669.
9. C.Balanis, Antenna Theory, Wiley & Sons, 1997, 942p.
10. A.A.Vertiy, S.P.Gavrilov, S.I.Tarapov, V.P.Shestopalov, Reports of Acad. of Sci. USSR, (1992) 323, N2, 270.
11. V.N.Derkach, R.V.Golovashchenko and A.S.Plevako, Proc. of 12th Int. Conf. "Microwave & Telecommunication Technology" (CriMiCo'2002). September 9-13, 2002, Sevastopol, Crimea, Ukraine. Sevastopol: "Weber" (2002) pp.548-549.